Nanoscale

Accepted Manuscript

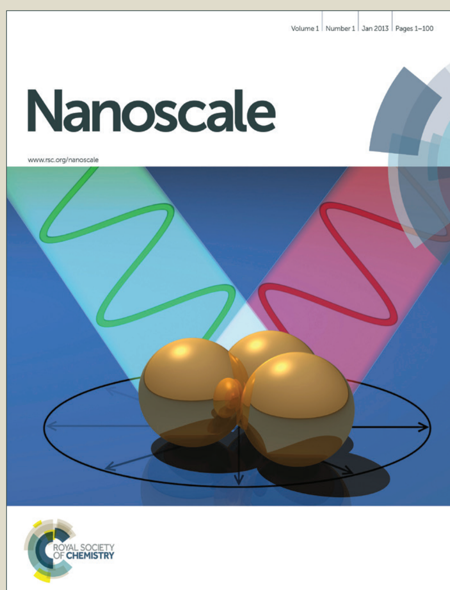

This is an *Accepted Manuscript*, which has been through the Royal Society of Chemistry peer review process and has been accepted for publication.

Accepted Manuscripts are published online shortly after acceptance, before technical editing, formatting and proof reading. Using this free service, authors can make their results available to the community, in citable form, before we publish the edited article. We will replace this *Accepted Manuscript* with the edited and formatted *Advance Article* as soon as it is available.

You can find more information about *Accepted Manuscripts* in the Information for Authors.

Please note that technical editing may introduce minor changes to the text and/or graphics, which may alter content. The journal's standard Terms & Conditions and the Ethical guidelines still apply. In no event shall the Royal Society of Chemistry be held responsible for any errors or omissions in this *Accepted Manuscript* or any consequences arising from the use of any information it contains.

ROYAL SOCIETY OF CHEMISTRY

www.rsc.org/nanoscale

Electrical-field-driven metal-insulator transition tuned with self-aligned atomic defects

Askar Syrlybekov[1,2,3], Han-Chun Wu[1,*], Ozhet Mauit[2], Ye-Cun Wu[1], Pierce Maguire[2], Abbas Khalid[2], Cormac Ó Coileáin[1,2], Leo Farrell[2], Cheng-Lin Heng[1], Mohamed Abid[4], Huajun Liu[5], li Yang[6], Hong-Zhou Zhang[2], Igor V. Shvets[2]

[1]*School of Physics, Beijing Institute of Technology, Beijing 100081, People's Republic of China*

[2]*CRANN, School of Physics, Trinity College, University of Dublin, Dublin 2, Ireland*

[3]*Nazarbayev University, 53 Kabanbay Batyr Avenue, Astana 010000, Kazakhstan*

[4]*KSU-aramco Center, King Saud University, Riyadh 11451, Saudi Arabia*

[5]*Institute of Plasma Physics, Chinese Academy of Sciences, Hefei 230031, People's Republic of China*

[6]*Electronic Engineering Institute, Hefei, 230037, People's Republic of China*

*Correspondence and requests for materials should be addressed to H.C.W. (wuhc@bit.edu.cn)

Recently, significant attention has been paid to the resistance switching (RS) behaviour in Fe_3O_4 and it was explained through the analogy of the electrical driven metal-insulator transition based on the quantum tunneling theory. Here, we propose a method to experimentally support this explanation and provide a way to tune the critical switching parameter by introducing self-aligned localized impurities through the growth of Fe_3O_4 thin films on stepped $SrTiO_3$ substrates. Anisotropic behavior in the RS was observed, where a lower switching voltage in the range of 10^4 V/cm is required to switch Fe_3O_4 from a high conducting state to a low conducting state when the electrical field is applied along the steps. The anisotropic RS behavior is attributed to a high density array of anti-phase boundaries (APBs) formed at the step edges and thus are aligned along the same direction in the film which act as a train of hotspots forming conduits for the resonant tunneling. Our experimental studies open an interesting window to tune the electrical-field-driven metal-insulator transition in strongly correlated systems.

Nanoscale Accepted Manuscript

Resistance switching (RS), in which the resistance of a device can be reversibly switched from a high conducting state to a low conducting state by an external electrical field, has recently attracted a great deal of attention. Due to the high switching speed, high densities, low operating voltages, and moreover structural simplicity, resistance random access memory (ReRAM) devices have been considered as potential candidates for nonvolatile memory. The RS phenomenon has been observed in many systems, including silicon,[1] sulfides,[2,3] organic materials,[4,5] and transition metal oxides[6].

Magnetite is an important transition metal oxide with exciting electronic, magnetic, and transport properties, such as a half-metallic character[7], high Curie temperature of 858 K [8,9], giant magnetization and large orbital moment in nanoscale magnetite[10,11], large transversal magnetoresistance (MR) [12,13], a spin filter effect[14], a spin valve effect[15,16], and a spin Seebeck effect[17]. As a strongly correlated system, Fe_3O_4 undergoes a metal–insulator transition at the Verwey temperature (T_V ~ 120 K) [18], which makes it a good candidate for ReRAM devices. Recently, the RS behaviour in epitaxial Fe_3O_4 thin films[19-23] and in polycrystalline Fe_3O_4 thin films[24] have been investigated by several groups. The effects of Joule heating[20], contact resistance[21], interfacial effect[22], and an external magnetic field[23] have been discussed. It has been found that RS in magnetite differs from RS in other transitional metal oxides where conductive filaments are formed due to dynamic percolation[25], or the migration of oxygen vacancies[26]. As RS in Fe_3O_4 can only be observed below the Verwey transition temperature and the switching field is 2 orders magnitudes lower than that for the Zener breakdown (10^6 V/cm), it is believed that RS in Fe_3O_4 is related to spin-charge ordering or the strongly correlated effect and it is explained by an effect analogous to an electrical-field-driven metal-insulator transition. However, the exact physics behind this is unclear. A recent experiment showed that an electrical field can slightly shift the Verwey temperature T_v but does not disrupt the Verwey transition itself[27]. Therefore, an electrical field-driven metal-insulator transition through modification of the Verwey transition can be ruled out. Another possible mechanism is based on a feedback effect of the current on the spin/charge ordering[28]. The key point of this mechanism is that the localized mid-gap states, introduced by

Nanoscale Accepted Manuscript

random impurities, act as hot spots where resonant tunneling occurs selectively. However, there has been no direct experimental confirmation of this. The main challenge in determining its validity is to introduce localized impurities to modify the quantum resonant tunneling process while keeping the properties of Fe_3O_4. Stepped substrates, where the height and width of the steps can be tuned through heat treatment[29], may offer an interesting platform to do this[30-32]. It has been experimentally suggested that, when Fe_3O_4 thin films are epitaxially grown on stepped and vicinal substrate surfaces[32-34], a high density of anti-phase boundaries (APBs) [35-38] will be formed along the step edges. Moreover, recent density functional theory (DFT) calculations showed that the electron states induced by APBs are strongly localized in the vicinity of these structural defects[39]. This prompted us to investigate RS in epitaxial Fe_3O_4 thin films on vicinal substrates.

In this work, we for the first time propose a method to experimentally support this explanation of RS in Fe_3O_4 and provide a way to tune the critical switching parameter by introducing self-aligned localized impurities through the growth of Fe_3O_4 thin films on stepped $SrTiO_3$ substrates. The surface of Fe_3O_4 thin films were characterized by atomic force microscopy (AFM) and their structural properties have been investigated by x-ray diffraction (XRD) and high resolution transmission electron microscopy (HRTEM). Anisotropic behavior in the RS was observed, where a lower switching voltage in the range of 10^4 V/cm is required to switch Fe_3O_4 from a high conducting state to a low conducting state when the electrical field is applied along the steps. The high density APBs formed at step edges act as hot spots which modify the quantum resonant tunneling process and decrease the switching voltage. Thus, our studies experimentally support the mechanism of the RS in Fe_3O_4 and open an interesting way to tune the electrical-field-driven metal-insulator transition in Fe_3O_4. Moreover, the filament is mainly confined in the step edges and since the step edges are all aligned along the same direction on the surface, an array of conducting conduits is formed in the film between the adjoining planar electrodes, such conduits can be switched on and off by the electric field. As the RS mechanism in Fe_3O_4 is different to the conventional

Nanoscale Accepted Manuscript

mechanism in other oxides, the total heat generation is also expected to be much less than in other RS devices.

Results

Sample preparation and characterization: In this work, we use single crystal $SrTiO_3$ (100) substrates with a miscut angle of 3° in the direction of <001>. To produce uniform and straight steps, the $SrTiO_3$ vicinal substrates were chemically cleaned and then annealed in air in a high temperature furnace at 1130°C for 3 hours[29-31]. The surface morphology of the $SrTiO_3$ vicinal substrates was examined with an Asylum Research MFP-3D AFM. **Figure 1a** shows a typical AFM image of a single crystal $SrTiO_3$ (100) vicinal substrate after annealing. Uniform and straight steps with atomically flat terraces are formed along the <010> direction. The steps height and terrace width estimated from height profile of AFM characterization are ~4 nm and ~83 nm respectively (**Figure S1**). To investigate the RS behaviour in Fe_3O_4, Fe_3O_4 thin films with a thickness of 95 nm were grown on the stepped $SrTiO_3$ substrates using an oxygen-plasma assisted MBE system (DCA MBE M600, Finland) with a base pressure of 5×10^{-10} torr. The Fe_3O_4 films were grown by electron beam evaporation of metallic iron (99.99%) in the presence of free oxygen radicals generated by an electron cyclotron resonance plasma source with a growth rate of 0.3 Å/s. The substrate temperature during growth was kept at 250°C. Details of the film growth are given elsewhere[10,13,17]. **Figure 1b** shows an AFM image of a 95 nm thick Fe_3O_4 film grown on the annealed stepped $SrTiO_3$ substrate. It is clear that the Fe_3O_4 film keeps the morphology of the substrate, as the dimensions of the steps and terraces did not change upon deposition of the magnetite. The steps remain parallel to the <010> direction. To further demonstrate the structural properties of the grown Fe_3O_4 thin films, **Figure 1c** shows a XRD ω-2θ scan, from 10 to 100 degrees, for a 95 nm thick Fe_3O_4 film on a stepped $SrTiO_3$ substrate. Only (100), (200), and (300) peaks for the $SrTiO_3$ substrate and (400) and (800) peaks for Fe_3O_4 film are observed indicating epitaxial growth of the Fe_3O_4. The peak positions for $SrTiO_3$ (200) and Fe_3O_4 (400) located at 46.4^0 and 43.2^0 respectively, which are consistent with the well-established values. To further demonstrate the stepped structure and epitaxial

Nanoscale Accepted Manuscript

nature of the Fe_3O_4 films at the step edges, we show in **Fig. 1d** a low magnification TEM image of the Fe_3O_4 thin film on the $SrTiO_3$ substrate demonstrating the epitaxial growth of Fe_3O_4 film on the stepped $SrTiO_3$ (100) substrate. Further evidence of the growth behaviour at the steps edges is shown in **Fig. 1e,** a HRTEM image at one of the step edges. It is clear that the Fe_3O_4 films were epitaxially grown on the $SrTiO_3$ substrates even at the step edges.

RS in magnetite: To investigate the effect of the steps on the RS behaviour in magnetite, we prepared devices with four probe contacts aligned either along the steps (AS) or perpendicular to the steps (PS). The two outer electrodes correspond to the source and drain leads respectively and the two inner electrodes are used to sense the voltage drop across the contacts. A voltage is applied to the source lead with the drain grounded, and current passing through the channel is measured. **Figure 2a** shows a scanning electron microscopy (SEM) image of a typical device with four probe contacts in a PS configuration, where the electrical field is applied along the steps. The steps between the contacts are uniform, continuous, and perpendicular to the electrodes. The gaps between source and drain and the two voltage sensing electrodes are 2.03 μm and 1.15 μm respectively. The devices in this study were fabricated using standard e-beam lithography (EBL) with a positive tone resist, PMMA A3 supplied by MicroChem Corp. After development, thick metal contacts consisting of Cu (7 nm)/Au (40 nm) were deposited by e-beam evaporation, where the 7 nm thick Cu layer served as an adhesion layer for the Au contacts. Moreover, Cu has a low contact resistance with Fe_3O_4 compared to Au[21]. After lift-off with acetone, macro-scale electrodes were prepared by UV lithography. Electric characterization of the samples was performed in a closed cycle refrigeration system, with a temperature range from 50 K to 300 K.

Figure 2b shows the temperature dependent resistance measured with a constant bias current of 10 μA. The Verwey transition for both device orientations was observed at a temperature of 122 K which is close to the bulk value[18], thus further indicating the high quality of the Fe_3O_4 thin films. Note, for Fe_3O_4 films on stepped substrates with a film thickness of 60 nm or less, the resistance of devices with contacts in the PS configure is

Nanoscale Accepted Manuscript

usually lower than that of devices with contacts in the AS configuration.[32] Here, to clearly distinguish the origin of the anisotropic switching, we measured the resistive switching behavior in Fe_3O_4 films with large thicknesses where the APBs effect on the long-range charge-orbital ordering is weaker as the distance between APBs or APB domain size increases with increasing film thickness.[38] No significant difference in the R-T curves was observed between two configurations which also helps us rule out any observed effect in the RS being due to difference in contact geometries. **Figures 2c** and **2d** show the I-V characterization for devices in both configurations measured at 90 K. Interestingly, we observed an anisotropic behaviour in RS, where a lower switching voltage is required to switch Fe_3O_4 from a high conducting state to a low conducting state when the electrical field is applied along the steps. The device with four contacts in PS configuration switches from a low conducting state to a high conducting state at a critical value (V_{SW}^{ON}) of 2.3 V which results in a sharp jump in current. Due to the effect of Joule heating, the device switches back to the low conducting state at a critical voltage (V_{SW}^{OFF}) of 2.27 V which is slight smaller than V_{SW}^{ON}. As the distance between the two sensing contacts is around 1.15 μm, the electrical switching field is estimated to be in the range of 10^4 V/cm, which is consistent with early reports[19-23]. However, for devices with four contacts in an AS configuration, V_{SW}^{ON} is around 3.5 V which is around 50% higher than that for devices with contacts in a PS configuration.

Field Code Changed

Figure 3a and **3b** plot the temperature dependent RS characterization for devices in both configurations. The switching voltage increases with decreasing temperature for both configurations. We summarized the temperature dependent V_{SW}^{ON} for both configurations in **Figure 3c**. Remarkably, anisotropic RS behavior was observed at all temperatures below Verwey temperature. Moreover, the difference in V_{SW}^{ON} between the PS and AS configurations increases with temperature decreasing. At 120 K, V_{SW}^{ON} for both configurations is almost the same but at 90 K, V_{SW}^{ON} for devices with four contacts in the AS configuration is almost 50% greater than that for devices with four contacts in the PS

Nanoscale Accepted Manuscript

configuration indicating steps significantly affect the RS behaviour in Fe_3O_4. To demonstrate the reliability and reproducibility of the RS behaviour in Fe_3O_4, a large number of switching cycles were performed on devices with contacts in the PS configure at 95 K. The V_{SW}^{ON} and V_{SW}^{OFF} for each cycle of such a device are shown in **Fig. 3d**. One can see that the device can survive upon more than 10^4 cycles and V_{SW}^{ON} and V_{SW}^{OFF} remain quite constant, showing that, the RS behaviour in our devices are reliable and reproducible.

Discussion

Before discussion of the mechanism behind the anisotropic RS, let us rule out that the effects due to the device geometry first. In this study, the gap between source and drain is 2.03 μm. If there is a small change in the gap between source and drain, this will not result in a significant change in V_{SW}^{ON}. This is verified by the fact that, at 120 K, V_{SW}^{ON} for both device configurations is almost the same. The current scattering at the steps can be ruled out as well as we use films with a thickness of 95 nm which is around 20 times larger than the height of the steps (4 nm). Indeed, R-T curves for both configurations show no significant difference (**Fig. 2b**). We have measured more than 10 Fe_3O_4 films with different thickness grown on stepped $SrTiO_3$ substrates. On each sample, we have at least 2 devices in PS configuration and 2 devices in AS configuration. Although the exact switching voltage of each device depends on film thickness and device geometry, we do observe similar anisotropic behavior with a lower switching voltage for devices with four contacts in the PS configuration. **Figure S2** shows the switching behavior of another Fe_3O_4 film grown on a stepped $SrTiO_3$ substrate. We also fabricated more than 20 devices using stepped MgO substrates. Similar anisotropic switching behavior has been observed. **Figure S3** shows typical RS for a 60 nm Fe_3O_4 film on stepped MgO substrates. Thus, our experimental observation is a general effect for Fe_3O_4 films on stepped substrates. For Fe_3O_4 films on flat substrates, we measured more than 20 samples. We did not observe the anisotropic behavior.

Nanoscale Accepted Manuscript

It has been shown by us and other research groups that when Fe_3O_4 are epitaxially on the stepped substrate, there is more than 75 % chance to form APBs at the step edges. Therefore, a high density APBs will be formed at the step edges[32-34] and the density of APBs at the step edges should be more than 50% higher than that on the terrace, which is consistent with our experimental observation, as the V_{SW}^{ON} for devices with four contacts in the AS configuration is almost 50% greater than for devices with four contacts in the PS configuration. Therefore, in our stepped Fe_3O_4 thin films, there are two kinds of APBs distributions: 1) A random distributed APBs on the terraces, as these APBs are a result of growth defects and the lattice mismatch between the film and the substrate[35-38]; 2) high density APBs at the step edges. As mentioned in the introduction, the electron states of the APBs are strongly localized in the energy gap of bulk Fe_3O_4.[39] Therefore, the APBs in the Fe_3O_4 thin films can be considered as localized impurities. We link our macroscopic I-V measurements to the theory suggested by Nagaosa *et al.* as follows. As schematically shown in **Figure S4**, when electrons tunnel through Fe_3O_4, the band structure of Fe_3O_4 with APBs will be spatially tilted by the potential energy gain $-eER$, where R is the real-space position and $-e$ is the electronic charge. The bottom of the conduction-band and the top of valence-band cross the energy =0 point at R_2 and R_1, respectively. The localized impurity state of the APBs is represented by the peak at $R=R_{APB}$, gives rise to the resonant tunneling. There are three critical lengths: 1) the correlation length ζ associated with the energy gap Δ, which describes the width of the filament path; 2) the tunneling length $\xi = 2\Delta / eE$, which is defined by Δ and the electric field E; and 3) the mean free path l. The condition to form a conductive filament is that the tunneling length is smaller than the correlation length, i.e. $\xi < \zeta$. In our stepped Fe_3O_4 thin films, we have two cases: 1) Random distributed localized impurities on the terraces; 2) self-aligned localized impurities at the step edges. The APBs can act as the nucleation centres for the non-equilibrium first-order metal-insulator phase transition and the current can more readily find a path along where these nucleation centres are densely populated compared with the other spatial regions. When an electrical field

Nanoscale Accepted Manuscript

applied along the steps, the filament will be formed at the step edges (**Fig. 4a**). Since the density of APBs at the step edges is higher than that on the terraces, a lower switching voltage is required to switch Fe_3O_4 from a high conducting state to a low conducting state. While when the electrical field is applied perpendicular to steps, the filament is quite similar to the case for flat Fe_3O_4 that is not compromised by one-dimensional defects. Therefore, our experiments support that the mechanism of the RS in Fe_3O_4 is the electrical field driven metal-insulator transition due to the feedback effect of the current on the spin/ charge ordering. It is worth pointing out that the RS in our system is more akin to a break-down type switching than the chemical-change-based switching discussed in Refs. 3 and 6. In the case when the electric field is applied along the steps the width of the conducting filament is of the order of nanometres. Once the filament is formed, the voltage potential across the sample diminishes and thus no additional filaments are created. Therefore, the total heat generation is expected to be much smaller than for other RS devices.

In conclusion, we investigated the RS in epitaxial Fe_3O_4 grown stepped substrates. Anisotropic RS behavior was observed and it is attributed to the APBs formed at step edges which work as hot spots. Our experiments confirm that the mechanism responsible for the RS in Fe_3O_4 is the electrical field driven metal-insulator transition due to the feedback effect of the current on the spin/ charge ordering. Our experimental studies may pave a way to tune the electrical field driven metal-insulator transition in strongly correlated systems.

Acknowledgements

This work was supported by Beijing Institute of Technology Research Fund Program for Young Scholars and National Plan for Science and technology (Nos. NPST 1598-02 and NPST 1466-02) of King Abdulaziz City for Science and Technology. H.C.W. and M.A. thank Saudi Aramco for the financial support (project No. 6600028398).

Methods

Nanoscale Accepted Manuscript

Sample preparation and characterization: $SrTiO_3$ vicinal substrates were chemically cleaned and then annealed in air in a high temperature furnace at 1130°C for 3 hours to produce uniform and straight steps. Fe_3O_4 thin films with a thickness of 95 nm were grown on the stepped $SrTiO_3$ substrates using an oxygen-plasma assisted MBE system (DCA MBE M600, Finland) with a base pressure of 5×10^{-10} torr. The surface morphology of the samples was examined with an Asylum Research MFP-3D AFM.

Device fabrication: The devices were fabricated using standard EBL with a positive tone resist, PMMA A3 supplied by MicroChem Corp. After development, Cu (7 nm)/Au (40 nm) were deposited as the metal contacts. After lift-off with acetone, macro-scale electrodes were prepared by UV lithography.

Author contributions

H.C.W. and I.V.S. conceived the study. O.M., L.F., and C.C. grew the sample. A.S. and M.A. fabricated the sample. P.M., A.K., and H.Z.Z. carried out the TEM measurements. H.C.W., C.L.H., and H.L. performed the transport measurements. L.Y. gave scientific advices. H.C.W. and Y.C.W. wrote the manuscript. All authors discussed the results and commented on the manuscript.

References

1. S. H. Jo, K.-H. Kim, W. Lu, *Nano Lett.* **2009**, 9, 870-874.

2. Z. M. Liao, C. Hou, Q. Zhao, D. S. Wang, Y. D. Li, D. P. Yu, *Small* **2009**, 5, 2377-2381.

3. R. Waser, M. Aono, *Nat. Mater.* **2007**, 6, 833-840.

4. Z. M. Liu, A. A. Yasseri, J. S. Lindsey, D. F. Bocian, *Science* **2003**, 302, 1543-1545.

5. H. K. Henisch, W. R. Smith, *Appl. Phys. Lett.* **1974**, 24, 589-591.

6. A. Sawa, *Materials Today* **2008**, 11, 28; and reference therein.

7. F. Walz, *J. Phys.: Condens. Matter.* **2002**, 14, R285.

8. M. Ziese, *Rep. Prog. Phys.* **2002**, 65, 143.

Nanoscale Accepted Manuscript

9. J. H. V. J. Brabers, F. Walz and H. Kronmuller, *J. Phys.: Condens. Matter.* **2002**, 12, 5437.

10. S. Arora, H. C. Wu, R. Choudhary, I. Shvets, O. Mryasov, H. Yao, and W. Ching, *Phys. Rev. B* **2008**, 77, 134443.

11. W. Q. Liu, Y. B. Xu, P. K. J. Wong, N. J. Maltby, S. P. Li, X. F. Wang, J. Du, B. You, J. Wu, P. Bencok, and R. Zhang, *Appl. Phys. Lett.* **2014**, 104, 142407.

12. A. Fernández-Pacheco, J. M. De Teresa, J. Orna, L. Morellon, P. A. Algarabel, J. A. Pardo, M. R. Ibarra, C. Magen, and E. Snoeck, *Phys. Rev. B* **2008**, 78, 212402.

13. H. C. Wu, R. Ramos, R. G. S. Sofin, Z. M. Liao, M. Abid, and I. V. Shvets, *Appl. Phys. Lett.* **2012**, 101, 052402.

14. Z. M. Liao, Y. D. Li, J. Xu, J. M. Zhang, K. Xia, and D. P. Yu, *Nano Lett.* **2006**, 6, 1087.

15. H. C. Wu, O. N. Mryasov, M. Abid, K. Radican, and I. V. Shvets, *Sci. Rep.* **2013**, 3, 1830.

16. X. Li, A. Gupta, G. Xiao, W. Qian, and V. Dravid, *Appl. Phys. Lett.* **1998**, 73, 3282.

17. R. Ramos, T. Kikkawa, K. Uchida, H. Adachi, I. Lucas, M. H. Aguirre, P. Algarabel, L. Morellon, S. Maekawa, E. Saitoh, and M. R. Ibarra, *Appl. Phys. Lett.* **2013**, 102, 072413.

18. Verwey, *Nature* **1939**, 144, 327.

19. S. Lee, A. Fursina, J.T. Mayo, C.T. Yavuz, V.L. Colvin, R.G. Sofin, I.V. Shvets, D. Natelson, *Nat. Mater.* **2008**, 7, 130-133.

20. A.A. Fursina, R.G.S. Sofin, I.V. Shvets, D. Natelson, *Phys. Rev. B* **2009**, 79, 245131.

21. A.A. Fursina, R.G.S. Sofin, I.V. Shvets, D. Natelson, *Phys. Rev. B* **2010**, 82, 245112.

22. A.A. Fursina, R.G.S. Sofin, I.V. Shvets, D. Natelson, *Phys. Rev. B* **2010**, 81, 045123.

23. A.A. Fursina, R.G.S. Sofin, I.V. Shvets, D. Natelson, *N. J. Phys.* **2012**, 14, 013019

24. R. V. Gudavarthy, A. S. Miller, E. W. Bohannan, E. A. Kulp, Z. He, J. A. Switzer, *Electrochimica Acta* **2011**, 56, 10550–10556.

25. S. H. Chang, J. S. Lee, S. C. Chae, S. B. Lee, C. Liu, B. Kahng, D. W. Kim, T. W. Noh, *Phys. Rev. Lett.* **2009**, 102, 026801.

Nanoscale Accepted Manuscript

26. Li He, Z. M. Liao, H.-C. Wu, X. X. Tian, D. S. Xu, G. L. W. Cross, G. S. Duesberg, I. V. Shvets, and D. P. Yu, *Nano Lett.* **2011**, 11, 4601.

27. J.J.I. Wong, A.G. Swartz, R. Zheng, W. Han, R.K. Kawakami, *Phys. Rev. B* **2012**, 86, 060409.

28. N. Sugimoto, S. Onoda, and N. Nagaosa, *Phys. Rev. B* **2008**, 78, 155104.

29. R. Verre, R.G.S. Sofin, V. Usov, K. Fleischer, D. Fox, G. Behan, H. Zhang, I.V. Shvets, *Surf. Sci.* **2012**, 606, 1815-1820.

30. R. K. Kawakami, Ernesto J. Escorcia-Aparicio, and Z. Q. Qiu, *Phys. Rev. Lett.* **1996**, 77, 2570.

31. I. V. Shvets, H. C. Wu, V. Usov, F. Cuccureddu, S. K. Arora, and S. Murphy, *Appl. Phys. Lett.* **2008**, 91, 023107.

32. H. C. Wu, A. Syrlybekov, O. Mauit, A. Mouti, C.Ó. Coileáin, M. Abid, M. Abid, I.V. Shvets, *Appl. Phys. Lett.* **2014**, 105, 132408.

33. S. K. Arora, R. G. S. Sofin, and I. V. Shvets, *Phys. Rev. B* **2005**, 72, 134404.

34. L. McGuigan, R.C. Barklie, R.G.S. Sofin, S.K. Arora, I.V. Shvets, *Phys. Rev. B* **2008**, 77,174424.

35. D. T. Margulies, F. T. Parker, M. L. Rudee, F. E. Spada, J. N. Chapman, P. R. Aitchison, and A. E. Berkovitz, *Phys. Rev. Lett.* **1997**, 79, 5162.

36. D. T. Margulies, F. T. Parker, F. E. Spada, R. S.Goldman, J. Li, R. Sinclair, A. E. Berkowitz, *Phys. Rev. B* **1996**, 53, 9175.

37. W. Eerenstein, T. T. M. Palstra, S. S. Saxena and T. Hibma, *Phys. Rev. Lett.* **2002**, 88, 247204.

38. H. C. Wu, M. Abid, B. S. Chun, R. Ramos, O. N. Mryasov, and I. V. Shvets, *Nano Lett.* **2010**, 10, 1132.

39. R. Arras, L. Calmels, and B. Warot-Fonrose, *Phys. Rev. B* **2010**, 81, 104422.

Nanoscale Accepted Manuscript

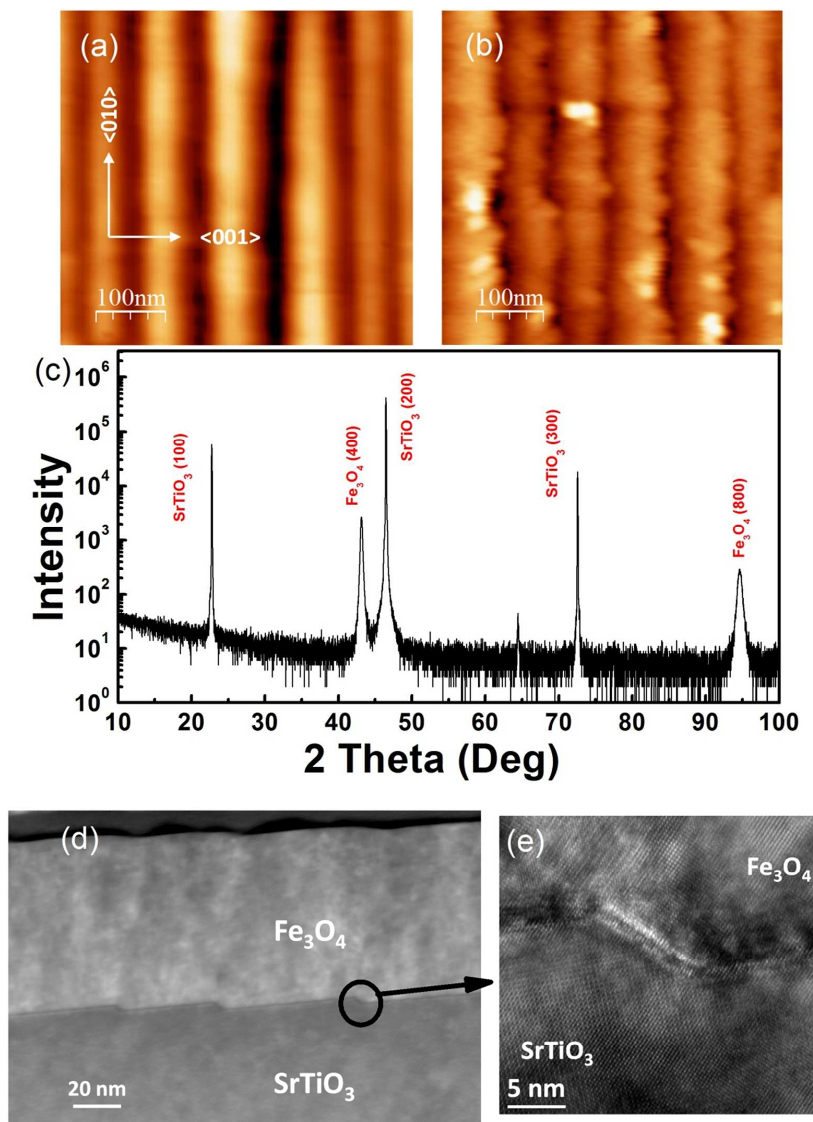

Figure 1. (a) AFM image of a $SrTiO_3$ substrate with a miscut angle of 3° annealed at 1130°C for 3 h (b) AFM image of 95 nm thick Fe_3O_4 deposited on a stepped $SrTiO_3$ substrate. The steps are parallel to the <010> direction. (c) XRD ω-2θ scan of 95 nm thick Fe_3O_4 film on a stepped $SrTiO_3$ (100) substrate. (d) Low magnification TEM image indicating the epitaxial growth of Fe_3O_4 film on a stepped $SrTiO_3$ (100) substrate. (e) HRTEM image indicating the epitaxial growth of the Fe_3O_4 film at the step edges.

Nanoscale Accepted Manuscript

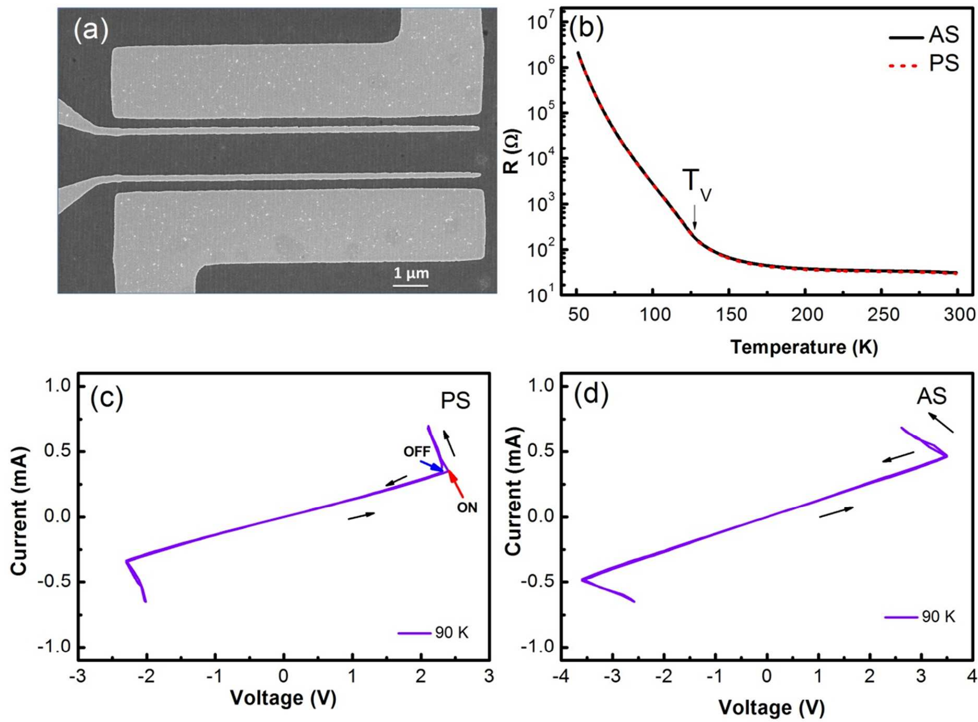

Figure 2. (a) SEM image of a device with four probe electrodes in PS configuration. (b) Temperature dependence of resistance measured with a constant current of 10μA. The Verwey transition is shown at T_V ~ 122 K. I-V measurement measured at 90 K for devices with four probe electrodes in PS (c) and AS (d) configuration.

Nanoscale Accepted Manuscript

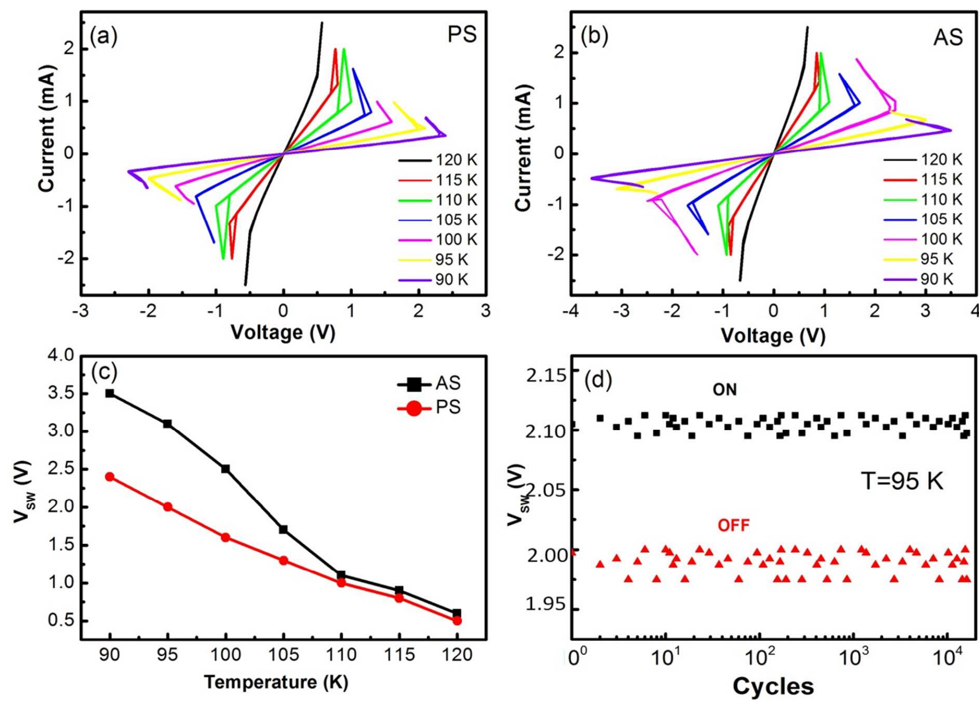

Figure 3. I-V measurements for temperatures between 120K – 90K, for devices with four probe electrodes in PS (a) and AS (b) configurations. (c) Difference in the switching voltage on for the electric field applied along the steps and perpendicular to steps. (d) V_{SW}^{ON} and V_{SW}^{OFF} for device with contacts in the PS configuration measured at 95 K.

Nanoscale Accepted Manuscript

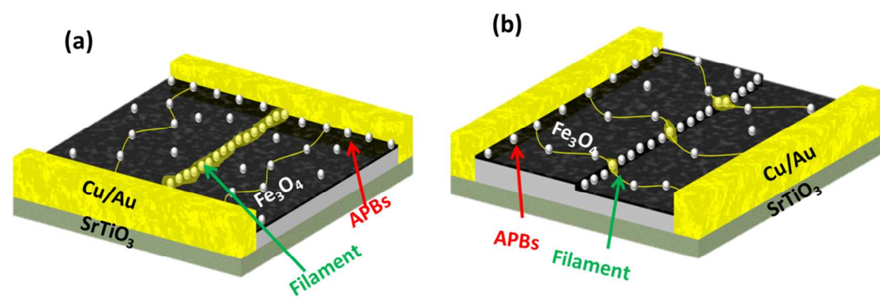

Figure 4. Schematic drawing of the filament formation for devices with four probe electrodes in both the PS (a) and AS (b) configurations.

Nanoscale Accepted Manuscript

Table of contents entry

An anisotropic resistance switching behavior has been observed in Fe_3O_4 thin films on stepped $SrTiO_3$ substrate.

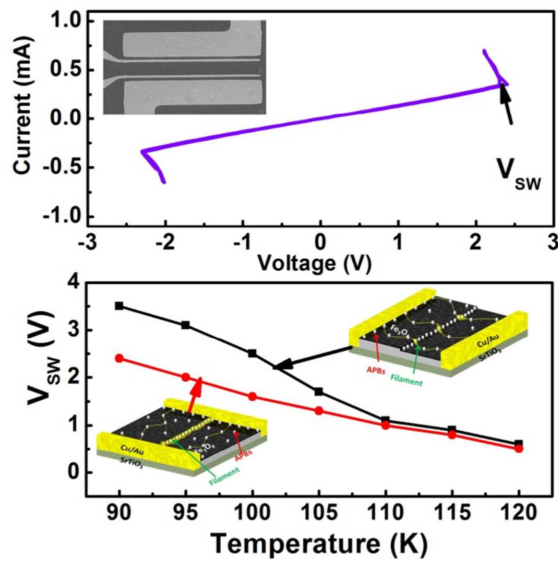

Nanoscale Accepted Manuscript